

Synthesis, Molecular, and Electronic Structure of $(\eta^8\text{-C}_8\text{H}_8)\text{Ln}(\text{scorpionate})$ Half-Sandwich Complexes: An Experimental Key to a Better Understanding of f-Element-Cyclooctatetraenyl Bonding[†]

Hanns-Dieter Amberger,^{*,‡} Frank T. Edelmann,^{*,§} Jochen Gottfriedsen,[§] Regine Herbst-Irmer,[⊥] Stefan Jank,[‡] Ulrike Kilimann,[⊥] Mathias Noltemeyer,[⊥] Hauke Reddmann,[‡] and Martina Schäfer[⊥]

Institut für Anorganische and Angewandte Chemie der Universität Hamburg, Martin-Luther-King-Platz 6, D-20146 Hamburg, Germany, Chemisches Institut der Otto-von-Guericke-Universität Magdeburg, Universitätsplatz 2, D-39106 Magdeburg, Germany, and Institut für Anorganische Chemie der Universität Göttingen, Tammannstrasse 4, D-37077 Göttingen, Germany

Received September 15, 2008

Synthetic routes leading to two series of $(\eta^8\text{-cyclooctatetraenyl})\text{lanthanide(III)}$ scorpionate “mixed sandwich” complexes are reported. The early lanthanide derivatives $(\text{COT})\text{Ln}(\text{Tp})$ ($\text{Ln} = \text{Ce}$ (**1**), Pr (**2**), Nd (**3**), Sm (**4**)) and $(\text{COT})\text{Ln}(\text{Tp}^{\text{Me}_2})$ ($\text{Ln} = \text{Ce}$ (**5**), Pr (**6**), Nd (**7**), Sm (**8**)) ($\text{COT} = \eta^8\text{-cyclooctatetraenyl}$, $\text{Tp} = \text{hydrotris}(\text{pyrazolyl})\text{borate}$, $\text{Tp}^{\text{Me}_2} = \text{hydrotris}(3,5\text{-dimethylpyrazolyl})\text{borate}$) were obtained by reacting the dimeric halide precursors $[(\text{COT})\text{Ln}(\mu\text{-Cl})(\text{THF})_2]_2$ with $\text{K}[\text{Tp}]$ or $\text{K}[\text{Tp}^{\text{Me}_2}]$, respectively. For the late lanthanide elements a different synthetic route was developed. The complexes $(\text{COT})\text{Ln}(\text{Tp})$ ($\text{Ln} = \text{Er}$ (**9**), Lu (**10**)) were made by the reaction of $(\text{Tp})\text{LnCl}_2(\text{THF})_{1.5}$ with equivalent amounts of $\text{K}_2\text{C}_8\text{H}_8$. All new compounds were isolated as intensely colored crystalline materials and fully characterized by elemental analyses and spectroscopic methods. The molecular structures of **4**, **5**, and **8** were elucidated by X-ray diffraction. The optical spectra of compounds **2** and **4–8** were run at room and low temperatures. From the spectra obtained, the underlying crystal field splitting patterns of complexes **2**, **4**, **6**, and **7** were derived and simulated by fitting the free parameters of a phenomenological Hamiltonian. The parameters used allow the estimation of the crystal field strengths experienced by the Ln^{3+} central ions and the insertion of complexes **2**, **4**, **6**, and **7** into empiric nephelauxetic and relativistic nephelauxetic series. Besides, the experimentally oriented non-relativistic and relativistic molecular orbital schemes of compound **6** were set up and compared with the results of previous model calculations on $[\text{Ln}(\text{COT})_2]^-$, $\text{Pa}(\text{COT})_2$, and $\text{U}(\text{COT})_2$.

1. Introduction

The potential applications of the lanthanide elements in catalysis, organic synthesis, diagnostics, and materials sciences had a major impetus on the rapid development of organolanthanide chemistry in recent years.^{1–3} Because of the large ionic radii of the lanthanides it is generally important to employ sterically demanding ancillary ligands

to kinetically stabilize the metal centers and to make isolation of well-defined organolanthanide species possible. For most of its history, this area has been largely dominated by cyclopentadienyl type ligands. However, in recent years

[†] Part 69 of the series “Electronic Structures of Organometallic Complexes of f Elements. For part 68, see: Amberger, H.-D., Reddmann, H. *Z. Anorg. Allg. Chem.* **2008**, *634*, 1542.

* To whom correspondence should be addressed. E-mail: frank.edelmann@ovgu.de.

[‡] Institut für Anorganische and Angewandte Chemie der Universität Hamburg.

[§] Chemisches Institut der Otto-von-Guericke-Universität Magdeburg.

[⊥] Institut für Anorganische Chemie der Universität Göttingen.

- (1) Review: Edelmann, F. T. *Complexes of Scandium, Yttrium and Lanthanide Elements, in Comprehensive Organometallic Chemistry III*, Crabtree, R. H., Mingos, D. M. P., Eds.; Elsevier: Oxford, 2006; pp 1–190.
- (2) (a) Yasuda, H. *Top. Organomet. Chem.* **1999**, *2*, 255. (b) Aspinall, H. C. *Chem. Rev.* **2002**, *102*, 1807. (c) Shibasaki, M.; Yoshikawa, N. *Chem. Rev.* **2002**, *102*, 2187. (d) Inanaga, J.; Furuno, H.; Hayano, T. *Chem. Rev.* **2002**, *102*, 2211. (e) Anwender, R. In *Applied Homogeneous Catalysis with Organometallic Compounds*; Cornils, B., Herrmann, W. A., Eds.; Wiley-VCH: Germany, 2002; Vol. 2, pp 974–1014. (f) Hong, S.; Marks, T. J. *Acc. Chem. Res.* **2004**, *37*, 673.
- (3) (a) Molander, G. A.; Dowdy, E. D. *Top. Organomet. Chem.* **1999**, *2*, 119. (b) Molander, G. A.; Romero, J. A. C. *Chem. Rev.* **2002**, *102*, 2161.

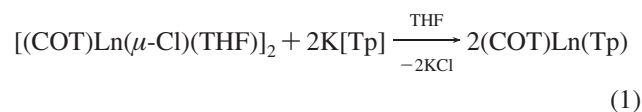
significant efforts have been directed toward the establishment of alternative ligand sets.^{4,5} These include other carbocyclic systems, as well as specially designed nitrogen donor ligands. Among the carbocyclic ring systems the large flat cyclooctatetraenyl ligand ($\text{C}_8\text{H}_8^{2-}$, = COT) plays a major role in organolanthanide chemistry.^{1–7} The synthesis of the first organolanthanide(III) complexes containing cyclooctatetraenyl complexes dates back to the year 1970, when Streitwieser et al. reported the preparation of highly air-sensitive anionic sandwich complexes of the type $[\text{Ln}(\text{COT})_2]^-$.^{9–11} The field of lanthanide cyclooctatetraenyl complexes has witnessed interesting developments in recent years.^{1,7} In particular, multifunctional nitrogen donor ligands have been developed, which fill the need of sterically saturating the large lanthanide centers. These include, among others, benzamidinates,^{12–15} guanidates,^{16–19} troponeimines,^{20,21} β -diketiminates,²² and scorpionates.^{23,24} Especially the latter have been demonstrated to be highly effective in

providing a well-defined ligand environment for the lanthanide elements. Numerous pyrazolylborates^{25,26} of both di- and trivalent lanthanide ions have been reported, and especially the former have led to an exciting derivative chemistry.^{27,28}

The combination of both a η^8 -COT ligand and a tridentate pyrazolylborate ligand in the coordination sphere leads to a class of thermally very stable *pseudo*-tetrahedrally coordinated organolanthanide complexes. We report here a systematic study of two series of “mixed sandwich” (η^8 -COT)lanthanide(III) scorpionate complexes containing the Tp (= hydrotris(pyrazolyl)borato) and the bulkier Tp^{Me2} (= hydrotris(3,5-dimethylpyrazolyl)borato) ancillary ligands. It has been established that these compounds play an important role in gaining a better understanding of f-element COT bonding. Part of this work has been published in preliminary form.^{29–31}

2. Results and Discussion

2.1. Syntheses. The starting materials $[(\text{COT})\text{Ln}(\mu\text{-Cl})(\text{THF})_2]_2$ were prepared from anhydrous LnCl_3 and $\text{K}_2\text{C}_8\text{H}_8$ according to the published method.^{32–34} Early lanthanide complexes of the type $(\text{COT})\text{Ln}(\text{Tp})$ are readily accessible, though in moderate yields, by treating the halide precursors $[(\text{COT})\text{Ln}(\mu\text{-Cl})(\text{THF})_2]_2$ with $\text{K}[\text{Tp}]$ according to eq 1.

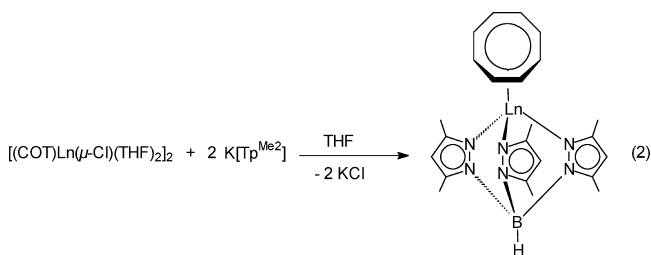


where **1**: Ln = Ce (pink-red), **2**: Ln = Pr (yellow-orange), **3**: Ln = Nd (green), **4**: Ln = Sm (red).

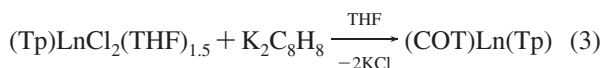
- (4) Edelmann, F. T. *Angew. Chem.* **1995**, *107*, 2647; *Angew. Chem., Int. Ed. Engl.* **1995**, *34*, 2466.
- (5) (a) Zakharov, L. N.; Struchkov, Y. T. *J. Organomet. Chem.* **1997**, *536–537*, 65. (b) Cotton, S. A. *Coord. Chem. Rev.* **1997**, *160*, 93. (c) Edelmann, F. T.; Freckmann, D. M. M.; Schumann, H. *Chem. Rev.* **2002**, *102*, 1851. (d) Piers, W. E.; Emslie, D. J. H. *Coord. Chem. Rev.* **2002**, *233–234*, 129.
- (6) Reviews: (a) Streitwieser, A., Jr.; Kinsley, S. A. In *Fundamental and Technological Aspects of Organo-f-Element Chemistry*; Marks, T. J., Fragalà, I. L., Eds.; NATO ASI Series; D. Reidel: Boston, 1985; Vol. 155, p 77. (b) Streitwieser, A.; Boussie, T. R. *Eur. J. Solid State Inorg. Chem.* **1991**, *28*, 399.
- (7) Edelmann, F. T. *New J. Chem.* **1995**, *19*, 535.
- (8) (a) Mares, F.; Hodgson, K. O.; Streitwieser, A., Jr. *J. Organomet. Chem.* **1971**, *28*, C24. (b) Mares, F.; Hodgson, K. O.; Streitwieser, A., Jr. *J. Organomet. Chem.* **1970**, *24*, C68. (c) Hodgson, K. O.; Mares, F.; Starks, D. F.; Streitwieser, A., Jr. *J. Am. Chem. Soc.* **1973**, *95*, 8650.
- (9) Jin, J.; Jin, S.; Jin, Z.; Chen, W. *J. Chem. Soc., Chem. Commun.* **1991**, 1328.
- (10) (a) Hodgson, K. O.; Raymond, K. N. *Inorg. Chem.* **1972**, *11*, 171. (b) Hodgson, K. O.; Raymond, K. N. *Inorg. Chem.* **1972**, *11*, 3030. (c) Mashima, K.; Takaya, H. *Tetrahedron Lett.* **1989**, *30*, 3697.
- (11) Shen, Q.; Chen, W.; Jin, Y. *Pure Appl. Chem.* **1988**, *60*, 1251.
- (12) (a) Duchateau, R.; van Wee, C. T.; Meetsma, A.; Teuben, J. H. *J. Am. Chem. Soc.* **1993**, *115*, 4931. (b) Duchateau, R.; van Wee, C. T.; Meetsma, A.; van Duijn, P. T.; Teuben, J. H. *Organometallics* **1996**, *15*, 2279. (c) Bambirra, S.; Bouwkamp, M. W.; Meetsma, A.; Hessen, B. *J. Am. Chem. Soc.* **2004**, *126*, 9182.
- (13) (a) Edelmann, F. T. *J. Alloys Compd.* **1994**, *207/208*, 182. (b) Edelmann, F. T. *Coord. Chem. Rev.* **1994**, *137*, 403. (c) Bailey, P. J.; Pace, S. *Coord. Chem. Rev.* **2001**, *214*, 91. (d) Coles, M. P. *Dalton Trans.* **2006**, 985. (e) Junk, P. C.; Cole, M. L. *Chem. Commun.* **2007**, 1579. (f) Edelmann, F. T. *Adv. Organomet. Chem.* **2008**, *57*, in print.
- (14) Roesky, P. W. *Z. Anorg. Allg. Chem.* **2003**, *629*, 1881.
- (15) Arndt, S.; Okuda, J. *Adv. Synth. Catal.* **2005**, *347*, 339.
- (16) (a) Zhou, Y. L.; Yap, G. P. A.; Richeson, D. S. *Organometallics* **1998**, *17*, 4387. (b) Lu, Z. P.; Yap, G. P. A.; Richeson, D. S. *Organometallics* **2001**, *20*, 706.
- (17) (a) Zhou, L.; Yao, Y.; Zhang, Y.; Xue, M.; Chen, J.; Shen, Q. *Eur. J. Inorg. Chem.* **2004**, 2167. (b) Luo, Y.; Yao, Y.; Shen, Q.; Sin, J.; Weng, L. *J. Organomet. Chem.* **2002**, *662*, 144.
- (18) (a) Chen, J.-L.; Yao, Y.-M.; Luo, Y.-J.; Zhou, L.-Y.; Zhang, Y.; Shen, Q. *J. Organomet. Chem.* **2004**, *689*, 1019. (b) Luo, Y.; Yao, Y.; Shen, Q.; Yu, K.; Weng, L. *Eur. J. Inorg. Chem.* **2003**, 318.
- (19) (a) Giesbrecht, G. R.; Whitener, G. D.; Arnold, J. J. *Chem. Soc., Dalton Trans.* **2001**, 923. (b) Pääväsäari, J.; Dezelah, C. L.; Back, D.; El-Kaderi, H. M.; Heeg, M. J.; Putkonen, M.; Niinistö, L.; Winter, C. H. *J. Mater. Chem.* **2005**, *15*, 4224.
- (20) (a) Roesky, P. W. *Inorg. Chem.* **1998**, *37*, 4507. (b) Roesky, P. W. *J. Organomet. Chem.* **2000**, *603*, 161.
- (21) (a) Meyer, N.; Zulus, A.; Roesky, P. W. *Organometallics* **2006**, *25*, 4179. (b) Meyer, N.; Roesky, P. W. *Dalton Trans.* **2007**, 2652. (c) Datta, S.; Gamer, T.; Roesky, P. W. *Organometallics* **2008**, 27, in print.

- (22) (a) Lee, L. W. M.; Piers, W. E.; Elsegood, M. R. J.; Clegg, W.; Parvez, M. *Organometallics* **1999**, *18*, 2947. (b) Bourget-Merle, L.; Lappert, M. F.; Severn, J. R. *Chem. Rev.* **2002**, *102*, 3031.
- (23) Trofimenko, S. *Scorpionates: The Coordination Chemistry of Poly-pyrazolylborate Ligands*; University College Press: London, 1999.
- (24) Trofimenko, S. *Polyhedron* **2004**, *23*, 197.
- (25) Review: Marques, N.; Sella, A.; Takats, J. *Chem. Rev.* **2002**, *102*, 2137.
- (26) (a) Hasinoff, L.; Takats, J.; Zhang, X. W.; Bond, P. H.; Rogers, R. D. *J. Am. Chem. Soc.* **1994**, *116*, 8833. (b) Lin, G. Y.; McDonald, R.; Takats, J. *Organometallics* **2000**, *19*, 1814. (c) Ferrence, G. M.; Arduengo, A. J.; Jockisch, A.; Kim, H.-J.; McDonald, R.; Takats, J. *J. Alloys Compd.* **2006**, *418*, 184. (d) Cheng, J.; Takats, J.; Ferguson, M. J.; McDonald, R. *J. Am. Chem. Soc.* **2008**, *130*, 1544.
- (27) (a) Hou, Z.; Yoda, C.; Koizumi, T.; Nishiura, M.; Wakatsuki, Y.; Fukuzawa, S.; Takats, J. *Organometallics* **2003**, *22*, 3586. (b) Galler, J. L.; Goodchild, S.; Gould, J.; McDonald, R.; Sella, A. *Polyhedron* **2004**, *23*, 253. (c) Morisette, M.; Haufe, S.; McDonald, R.; Ferrence, G. M.; Takats, J. *Polyhedron* **2004**, *23*, 263.
- (28) (a) Domingos, A.; Lopes, I.; Waerenborgh, J. C.; Marques, N.; Lin, G. Y.; Zhang, X. W.; Takats, J.; McDonald, R.; Hillier, A. C.; Sella, A.; Elsegood, M. R.; Day, V. W. *Inorg. Chem.* **2007**, *46*, 9415. (b) Zimmermann, M.; Takats, J.; Kiel, G.; Törnroos, K. W.; Anwander, R. *Chem. Commun.* **2008**, 612.
- (29) (a) Masino, A. P. Ph. D. Thesis, University of Alberta, Alberta, Canada, 1978. (b) Kilimann, U.; Edelmann, F. T. *J. Organomet. Chem.* **1994**, *469*, C5. (c) Kilimann, U.; Edelmann, F. T. *J. Organomet. Chem.* **1994**, *469*, C29.
- (30) Amberger, H.-D.; Edelmann, F. T. *J. Organomet. Chem.* **1996**, *508*, 275.
- (31) Jamerson, J. D.; Masino, A. P.; Takats, J. *J. Organomet. Chem.* **1974**, *65*, C33.
- (32) Warren, K. D. *Struct. Bonding (Berlin)* **1976**, *33*, 97; and references therein.
- (33) Wetzel, T. G.; Roesky, P. W. *Organometallics* **1998**, *17*, 4009.
- (34) Kilimann, U.; Herbst-Irmer, R.; Stalke, D.; Edelmann, F. T. *Angew. Chem.* **1994**, *106*, 1684; *Angew. Chem., Int. Ed. Engl.* **1994**, *33*, 1618.

Isolation of **1–4** was achieved by extraction with toluene followed by washing with *n*-hexane (**1–3**) or recrystallization from toluene (**4**). The intensely colored compounds are highly air-sensitive. The pink-red cerium derivative **1** is the most air-sensitive species. In the presence of traces of oxygen the solid material undergoes an immediate color change to purple and brown. The reaction depicted in eq 1 works equally well with the sterically more demanding hydrotris(3,5-dimethylpyrazol-1-yl)borate ligand. Treatment of $[(\text{COT})\text{Ln}(\mu\text{-Cl})(\text{THF})_2]_2$ with 2 equiv of $\text{K}[\text{Tp}^{\text{Me}_2}]$ proceeded cleanly to afford the brightly colored complexes **5–8** in moderate yields (eq 2). Like the ring-unsubstituted derivatives, the compounds **5–8** are very air-sensitive and exhibit high melting/decomposition points. Because of the presence of six methyl groups they are better soluble in aromatic hydrocarbons. where **5**: Ln = Ce (pink), **6**: Ln = Pr (yellow), **7**: Ln = Nd (green), **8**: Ln = Sm (purple).



While the preparations outlined in eqs 1 and 2 work well with the early members of the lanthanide series, the synthesis is not as clean in the case of the late lanthanide elements. Thus, a second synthetic route has been developed which involves the reaction of $(\text{Tp})\text{LnCl}_2(\text{THF})_{1.5}$ with stoichiometric amounts of $\text{K}_2\text{C}_8\text{H}_8$ as shown in eq 3. Using this method we succeeded in preparing the late lanthanide derivatives $(\text{COT})\text{Er}(\text{Tp})$ (**9**) and $(\text{COT})\text{Lu}(\text{Tp})$ (**10**).



where **9**: Ln = Er (pink), **10**: Ln = Lu (colorless).

The complexes **9** and **10** can be readily isolated by crystallization after filtration to remove KCl. They too are sensitive to air and water and are soluble in toluene, THF, and pyridine. Experimental details for the synthesis and characterization of all complexes, as well as a discussion of the IR and NMR spectroscopic results, are provided in the Supporting Information.

2.2. Crystal Structures. The molecular structures of the complexes **4**, **5**, and **8** were determined by single-crystal X-ray diffraction. The molecular structures are shown in Figures 1–3. Crystal data as well as important bond lengths (Å) and angles (deg) are provided in the Supporting Information, Tables SI-1 and SI-2.

The crystal structure determination of **4** confirmed the presence of an unsolvated “sandwich complex” containing a COT ligand and a tridentate pyrazolylborate anion facing each other. The Sm atom is coordinated in a distorted *pseudo*-tetrahedral fashion by the center of the η^8 -coordinated COT ring and three nitrogens of the Tp ligand. The mean Sm–N

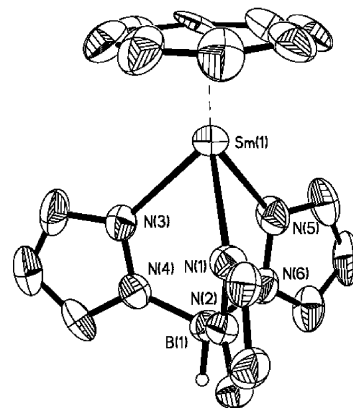


Figure 1. Crystal structure of **4**. Hydrogen atoms and second position of the COT group are omitted for clarity.

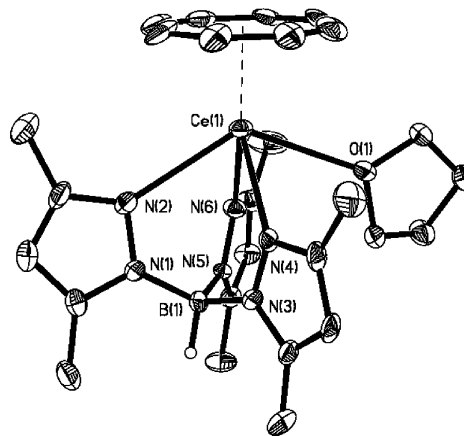


Figure 2. Crystal structure of **5**. Hydrogen atoms and second position of the COT and the THF group are omitted for clarity.

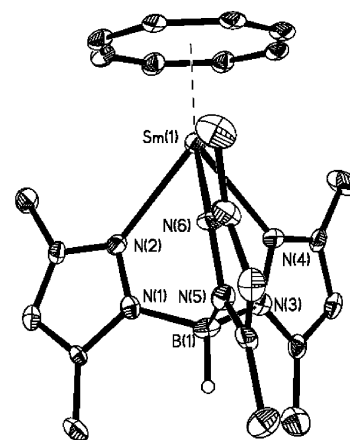


Figure 3. Crystal structure of one molecule of **8**. Hydrogen atoms and second position of the COT group are omitted for clarity.

distance is 2.482(7) Å and the average N–Sm–N angle is 75.8(2)°. The Sm–C distances range from 2.56(2) to 2.66(2) Å. With 1.538(11) Å the average B–N distance is nearly identical with that in $\text{Sm}(\text{Tp})_3$ (1.555(10) Å). Compound **8** crystallizes with two nearly identical crystallographic independent molecules in the asymmetric unit. The structure is very similar to that of **4**. Here the mean Sm–N distance is 2.543(8) Å and the average N–Sm–N angle is 77.8(2)°, while the average B–N distance equals 1.542(11) Å. The Sm–C distances range from 2.60(2) to 2.79(4) Å. The

slightly longer bond lengths compared to the values of **4** can be explained by the lower data collection temperature for **8**. In **5** an additional THF molecule is attached to the Ce atom. This additional ligand leads to a lowering of the symmetry in the coordination of the Tp^{Me_2} ligand. In contrast to **4** and **8** there is no longer a local 3-fold axis. The bond lengths Ce(1)–N(6) (2.570(3)) and Ce(1)–N(4) (2.573(3)) are nearly identical and equivalent to the Sm–N bond lengths of **4** and **8** taking the larger ionic radius of Ce^{3+} into account. However, the Ce(1)–N(2) bond (2.768(3)) is nearly 0.2 Å longer. Compared to the Sm compounds also the mean N–Ce–N angle (73.6(2)°) is smaller. The Ce(1)–O(1) bond (2.805(5)) is longer than in CeI(COT)(THF)₃^{10c} (2.593) or [CeCl(COT)(THF)₂]₂^{10a} (2.583). The Ce–C distances range from 2.69(1) to 2.80(1) Å

2.3. Electronic Structures of Selected (COT)Ln(scorpionates). Symmetry Considerations, Theory, Procedure, and Definitions. *N*-membered aromatic ring ligands with $N \geq 7$ are equivalent to cycles from the *f* electrons perspective.³² Therefore, not only [Ln(COT)₂][−] anions of *D*_{8h} and *D*_{8d}, but also related compounds of *D*₈ symmetry are centrosymmetric from the *f* electrons perspective, and therefore *f*–*f* transitions are strictly Laporte forbidden. Examples of the above-mentioned types of symmetries are [Li(diglyme)₂][Ln(1,4-R₂C₈H₆)₂] (Ln = Nd, Sm; R = *ortho*-(dimethylsilyl)-*N,N*-dimethylaniline)³³ (*D*_{8h}), [K(diglyme)][Ce(COT)₂]¹⁰ (*D*_{8d}) and Ce[1,3,6-(Me₃Si)₃C₈H₅]₂ (*D*₈, although here the rings are not strictly parallel).³⁴ For this reason optical spectra of full sandwich complexes of the stoichiometry [Ln(COT)₂][−] are of vibronic nature,^{8,35} and thus, it is extremely difficult to extract the underlying CF splitting patterns of these compounds from optical spectra. In neutral half-sandwich complexes of the stoichiometry (COT)Ln^{III}(L) the *f* electrons are exposed to an effective CF of approximate *C*_{∞v} symmetry if the CF splitting effects associated with the ligand L[−] may be safely neglected. The point group *C*_{∞v} does not include the symmetry operation of an inversion, and thus, *f*–*f* transitions are allowed by symmetry and are also observed in the optical spectra. The main problem, however, is to select systems where the above-mentioned condition is fulfilled. Low CF strengths are usually associated with I[−], THF, β-diketonato, and dithiophosphinato ligands.^{36,37} However, the low temperature absorption spectra of (COT)LnI(THF)₃ (Ln = Pr, Nd, Sm), obtained from pellets, differ noticeably from those of (glassy frozen) 2-MeTHF solutions,³⁸ thus indicating that the coordination sphere around the Ln³⁺ ion is somewhat different in the two media. Powdered (COT)Ln(Tp) or (COT)Ln(Tp^{Me2}) complexes exhibit nearly identical optical spectra as the corresponding (COT)LnI(THF)₃^{38,39} but the solvent effects are less pronounced (*vide infra*). The similarity of the spectra led us to the conclusion that the main contribution to the CF splitting effects of both types of

compounds is nearly exclusively because of the COT ligand, and the influence of the Tp or Tp^{Me2} ligands may be safely neglected.^{31,40,41}

This conclusion was recently supported by an analysis of the experimental CF splitting pattern (mainly based on the “polarized” luminescence spectrum of an oriented single crystal) of homoleptic Pr(Tp)₃.⁴² This analysis led to a global CF strength (*vide infra*) of 581 cm^{−1} experienced by the Pr³⁺ central ion⁴² and thus to a much lower individual CF strength for one single Tp ligand, whereas that of the COT ligand in the [Pr(COT)]⁺ moiety (neglecting the influence of the Tp or Tp^{Me2} ligand, respectively) is in the range of 1250 cm^{−1}.^{31,40} As the CF strength of the COT ligand is much greater than that of the Tp ligand (with comparable average Ln–N distances in Sm(Tp)₃⁴³ and compound **8**, respectively) it is to a certain degree justified to split the influence of the COT and scorpionate ligands into a main field of *C*_{∞v} and a perturbation field of *C*_{3v} symmetry. The weak perturbation of the main field caused by the trigonal field of the N atoms of the scorpionate ligand leads to an insignificant splitting of 2-fold degenerate CF states of *fⁿ* systems (*n* even)^{31,40} which is adequately considered by introducing the CF parameter B₆⁰ (*vide infra*).⁴⁰ In case of *fⁿ* systems with an odd number of *f* electrons the perturbing field does not split the Kramers pairs but its influence is partly absorbed by a slight variation of the CF parameters B₀², B₀⁴, B₀⁶ of the *C*_{∞v} main field, leading to poorly reduced rms deviations (*cf.* Table 3, *vide infra*). Assuming a CF of *C*_{∞v} symmetry the multiplets ^{2S+1}L_J of the free Ln³⁺ central ions (with an *fⁿ* configuration) are split into a number of CF states, the wave functions of which are described to first order by |±M_J⟩ (*M_J* integral for even *n*; *M_J* half-integral for odd *n*). If the wave function of an initial state is given by |±M_J⟩, forced electric dipole transitions are allowed to terminal levels with *M_J*′ = *M_J* and *M_J* ± 1⁴⁴ and thus strong signals for transitions to these states are expected. However, because of the trigonal distortion of the *C*_{∞v} main field, additional transitions become weakly allowed. The energy levels within *fⁿ* configuration in *C*_{∞v} symmetry can be written in terms of the atomic free ion (*H*_{FI}) and crystal field (*H*_{CF}) Hamiltonians as follows:

$$H = H_{\text{FI}} + H_{\text{CF}} \quad (4)$$

where

- (40) Amberger, H.-D.; Jank, S.; Reddmann, H.; Edelmann, F. T. *Mol. Phys.* **1996**, *88*, 1439.
 (41) Unrecht, B.; Jank, S.; Reddmann, H.; Amberger, H.-D.; Edelmann, F. T.; Edelstein, N. M. *J. Alloys Compd.* **1997**, *250*, 383.
 (42) Amberger, H.-D.; Reddmann, H.; Apostolidis, C.; Kanellakopulos, B. *Z. Anorg. Allg. Chem.* **2003**, *629*, 147.
 (43) Apostolidis, C.; Rebizant, J.; Walter, O.; Kanellakopulos, B.; Reddmann, H.; Amberger, H.-D. *Z. Anorg. Allg. Chem.* **2002**, *628*, 2013.
 (44) Görlner-Walrand, C.; Binnemans, K. In *Rationalization of Crystal Field Parametrization*; Gschneidner, K. A., Jr.; Eyring, L., Eds.; Handbook on the Physics and Chemistry of Rare Earths; Elsevier Science B.V.: Amsterdam, 1996; Vol. 23, Chapter 155, and references therein.

- (35) Mowery, R. L. *Diss. Abstr. Int.* **1977**, *37*, 5112B.
 (36) Wagner, W.; Edelstein, N.; Whittaker, B.; Braun, D. *Inorg. Chem.* **1977**, *16*, 1021; and references therein.
 (37) Pinkerton, A. A.; Amberger, H.-D.; unpublished results.
 (38) Amberger, H.-D.; Edelmann, F. T.; unpublished results.
 (39) Amberger, H.-D.; Jank, S.; Edelmann, F. T. *J. Organomet. Chem.* **1998**, *559*, 209.

$$H_{\text{FI}} = \sum_{k=0,2,4,6} f_k F^k(\text{nf}, \text{nf}) + a_{\text{SB}} \zeta_{4f} + \alpha L(L+1) + \beta G(G_2) + \gamma G(G_7) + \sum_{i=2,3,4,6,7,8} t_i T^i + \sum_{k=0,2,4} m_k M^k + \sum_{k=2,4,6} p_k P^k \quad (5)$$

(see refs 44 (p 167), 45) and

$$H_{\text{CF}}(C_{\infty v}) = B_o^2 C_o^{(2)} + B_o^4 C_o^{(4)} + B_o^6 C_o^{(6)} \quad (6)$$

(see ref 44 (p.245)).

The $F^k(\text{nf}, \text{nf})$'s and ζ_{4f} represent, respectively, the radial parts of the electrostatic and spin-orbit interactions between f electrons, while f_k and a_{so} are the angular parts of these interactions. α , β , and γ are the parameters associated with the two-body effective operators of configuration interaction, and the T^i 's are the corresponding three-body effective operators. The M^k parameters represent the spin-spin and spin-other-orbit interactions, while the P^k parameters arise from electrostatic spin-orbit interactions with higher configurations.⁴⁵ The CF interaction for the above symmetries is represented by the B_q^k parameters and the tensor operators $C_q^{(k)}$ (see ref 44 (p 245)).

Organometallic π complexes of f elements usually do not have good enough crystallizing properties to grow large single crystals necessary for polarized absorption measurements, and additionally the principal rotation axes of the individual molecules in the unit cell are frequently not aligned. Even if they were aligned, in the case of triclinic or monoclinic crystal systems it is difficult to orient these rotation axes with respect to outer homogeneous or vector fields.^{46,47} For this reason, the optical properties of f element organyls are usually studied in solution or as pellets, thus missing the additional information obtainable from optical polarization measurements. An elegant way out of these difficulties would be to perform magnetic circular dichroism (MCD) measurements⁴⁸ of (glassy frozen) solutions of f^n systems with an even number of f electrons.^{48,49} However, this method works only well if the initial state of the observed "cold" transitions^{50,51} or the terminal state of "hot" transitions are described by $|0\rangle$.⁵⁰ This situation is met in the case of all Eu^{III} (see ref 52, p 242) and a number of molecular Pr^{III} compounds.^{50,53-55} An additionally very helpful case is met in the case of highly symmetric Pr^{III} compounds, where the

crystal field ground state and the usually fluorescing level arising from $^3\text{P}_0$ are of different symmetry. In this situation, the different selection rules for absorption and luminescence transitions predict bands which are only observed in either the absorption or the luminescence spectrum, respectively, and signals which are observed in both types of spectra. If these predictions are met by the spectra, an experimental assignment of the terminal states of the observed transitions is possible, in principle (vide infra).⁴⁰ If the above-mentioned experimental methods do not work, one has to make use of the results of model calculations. A very powerful method is the so-called "calculational assignment".⁵⁶⁻⁵⁸ This method is based on the finding that the CF parameters of the Ln compound of interest do not differ strongly from those of the same compound of the neighboring element (see refs 44, Table 8, and 59). Besides, this method assumes that the free ion parameters of the Ln compound of interest are comparable to those of a chemically closely related Ln compound.⁵⁶⁻⁵⁸ Thus, the roughly estimated CF and free ion parameters are inserted into the energy matrix of the f^n system of concern. The diagonalization of this matrix leads frequently to eigenvalues which are comparable to the experimental energies of CF levels, which are assigned according to the results of the CF calculation.

In the case of classes of compounds, however, where no parametric CF analyses have been performed, it may be helpful to extract a first rough set of parameters from the more or less reliable results of quantum chemical calculations (of very different degrees of sophistication) on the compound of interest. The free parameters of a phenomenological Hamiltonian (eqs 5, 6) are fitted by least-squares routines to the (experimentally or computationally assigned) experimental energies of CF levels. To reduce the number of free parameters, the free ion parameters α , β , γ , T^i , M^k , and P^k used in the previous CF analyses of organometallic Ln^{III} compounds or $\text{LaCl}_3\text{:Ln}^{3+60}$ are adopted. The goodness of the fit is discussed in terms of the reduced rms deviation (σ), which is given by the relation

$$\sigma = \sqrt{\sum (E_{\text{exp}} - E_{\text{calc}})^2 / (n - p)} \quad (7)$$

(see ref 44 (p 164)).

(45) Carnall, W. T.; Crosswhite, H.; Crosswhite, H. M.; Hessler, J. P.; Edelstein, N. M.; Conway, J. G.; Shalimoff, G. V.; Sarup, R. *J. Chem. Phys.* **1980**, *72*, 5089.

(46) Nordén, B. *Appl. Spectrosc. Rev.* **1978**, *14*, 157.

(47) Rodger, R.; Nordén, B. *Circular Dichroism and Linear Dichroism*; Oxford University Press: Oxford, 1997; and references therein.

(48) Piepho, S. B.; Schatz, B. N. *Group Theory in Spectroscopy (With Applications to Magnetic Circular Dichroism)*; John Wiley & Sons, Inc.: New York, 1983; p 88.

(49) Görller-Walrand, C.; Behets, M.; Porcher, P.; Laursen, I. *J. Chem. Phys.* **1985**, *83*, 4329.

(50) Amberger, H.-D.; Jahn, W.; Edelstein, N. M. *Spectrochim. Acta* **1985**, *41A*, 465.

(51) Amberger, H.-D.; Fischer, R. D.; Yünlü, K. *Organometallics* **1986**, *5*, 2109.

(52) Dieke, G. H. *Spectra and Energy Levels of Rare Earth Ions in Crystals*; Interscience: New York, 1968; and references therein.

(53) Amberger, H.-D.; Schulz, H.; Reddmann, H.; Jank, S.; Edelstein, N. M.; Qian, C.; Wang, B. *Spectrochim. Acta* **1996**, *52A*, 429.

(54) Amberger, H.-D.; Hagen, C.; Shalimoff, G. V.; Edelstein, N. M. *Spectrochim. Acta* **1992**, *48A*, 1107.

(55) Guttenberger, C.; Amberger, H.-D. *J. Organomet. Chem.* **1997**, *545-546*, 601.

(56) Amberger, H.-D.; Reddmann, H.; Guttenberger, C.; Unrecht, B.; Zhang, L.; Apostolidis, C.; Walter, O.; Kanellakopulos, B. *Z. Anorg. Allg. Chem.* **2003**, *629*, 1522.

(57) Amberger, H.-D.; Reddmann, H.; Jank, S.; Lopes, M. I.; Marques, N. *Eur. J. Inorg. Chem.* **2004**, 98.

(58) Schulz, H.; Hagen, C.; Reddmann, H.; Amberger, H.-D. *Z. Anorg. Allg. Chem.* **2004**, *630*, 268.

(59) Schulz, H.; Reddmann, H.; Amberger, H.-D.; Kanellakopulos, B.; Apostolidis, C.; Rebizant, J.; Edelstein, N. M. *J. Organomet. Chem.* **2001**, *622*, 19.

(60) Carnall, W. T.; Crosswhite, H.; Crosswhite, H. M. Energy level structure and transition probabilities in the spectra of the trivalent lanthanides in LaF_3 ; ANL Report: 1977, unpublished; Appendix I, Table 1.

(61) Auzel, F.; Malta, O. L. *J. Phys. (Paris)* **1983**, *44*, 201.

where E_{exp} and E_{calc} are the experimental and calculated energy levels, respectively. n is the number of experimental energy levels and p the number of varied parameters.

The parameter $N_{\nu}/\sqrt{4\pi}$ which is defined by

$$N_{\nu}/\sqrt{4\pi} = \sqrt{\sum_{k,q} (B_q^k)^2 / (2k+1)} \quad (8)$$

(see ref 61) is considered as a relative measure of the global crystal field strength experienced by the Ln^{3+} central ion, where the B_q^k 's represent the phenomenological CF parameters used in the fit.

The nephelauxetic parameter β is defined as $\beta_{\text{F}} = F^2(\text{complex})/F^2(\text{free ion})^{62}$ (or alternatively as $\beta_{\text{E}} = E^1(\text{complex})/E^1(\text{free ion})^{62}$ where E^1 is a Racah parameter), the relativistic nephelauxetic parameter β' as $\beta' = \zeta_{4f}(\text{complex})/\zeta_{4f}(\text{free ion})^{63}$ and the covalency \sqrt{b} of the f-like wave function $|\phi_f\rangle = \sqrt{1-b} |4f\rangle - \sqrt{b} |\phi_{\text{ligands}}\rangle$ approximately by

$$\sqrt{b} = \sqrt{(1 - \beta_{\text{E}})/2} \quad (9)$$

(see ref 64) where $|4f\rangle$ are the unperturbed f functions and $|\phi_{\text{ligands}}\rangle$ the wave functions of the ligands. Unfortunately, the above-mentioned free ion values are only known for Ce^{3+65} and Pr^{3+66} and thus reliable β , β' , and \sqrt{b} values can only be given for Ce^{III} and Pr^{III} compounds. In case of the remaining compounds, the nephelauxetic parameter β_{J} is roughly estimated by the following relation as given by Jørgensen:⁶²

$$\nu - \nu_{\text{aquo}} = d\sigma - (1 - \beta_{\text{J}}) \times \nu_{\text{aquo}} \quad (10)$$

where ν denotes the wavenumber of a certain transition of the Ln complex of interest, ν_{aquo} the same transition of the corresponding $[\text{Ln}(\text{H}_2\text{O})_9]^{3+}$ ion, and $d\sigma$ is the energy difference of the ground multiplet barycenters of both compounds. Alternatively, empiric nephelauxetic series are built up by simply ordering the compounds of interest according to their F^2 or E^1 values, respectively.^{62,63}

If ligand orbitals of f element organyls have comparable energies as higher f orbitals, covalent interaction and thus the ligand fraction of these higher f-like wave functions increases. For this reason, the interelectronic repulsion and the spin-orbit coupling (considered by F^2 , F^4 , F^6 , and ζ_{4f} , respectively) is noticeably reduced for higher multiplets. The phenomenological Hamiltonian, however, assumes constant F^2 , F^4 , F^6 , and ζ_{4f} parameters throughout the f^n configuration (cf. eq 5). For this reason, calculated CF energies of higher multiplets are by hundreds of wavenumbers greater than the experimental ones^{59,67,68} (although the calculated CF splitting referred to the energetic barycenter of the multiplet of consideration is adequate), and thus, the CF states arising from these higher multiplets may not be considered in the fit. Hayes and Edelstein calculated the MO schemes (in the

f range) of $\text{U}(\text{COT})_2$ by means of the Mulliken-Helmholtz-Wolfsberg approximation, and fitting the CF parameters B_0^2 , B_0^4 , and B_0^6 of the spin-free f^1 system to this MO scheme, they estimated the CF parameters of this compound.^{69,70} In ref 71 an inverse procedure was suggested to check the results of previous, and as a criterion for the accuracy of future, quantum chemical model calculations. There, the eigenvalues of an energy matrix of the spin-free f^1 system, into which the CF parameters of a parametric analysis of the compound of interest had been inserted, were defined as the experimentally based non-relativistic MO scheme of this compound in the f range.⁷¹ Likewise, the eigenvalues of an energy matrix of the real f^1 system, into which the spin-orbit coupling as well as the CF parameters had been inserted, were defined as the experimentally based relativistic MO scheme of this compound in the f range.⁷²

2.4. Optical and Magnetochemical Results and Their Interpretation. (a) $(\text{COT})\text{Ce}[\text{Tp}^{\text{Me}_2}](\text{THF})$ (5). The optical properties of numerous salts and solids, but only of few organometallics of $\text{Ce}^{\text{III}73-77}$ have been studied during the last decades leading to the following results and definitions. Ce^{III} compounds exhibit sharp signals of f-f origin in the FIR/IR (ref 52 p 192),^{74,75} and Raman spectra^{75,77,78} (the intensities of which are strongly dependent on the temperature) and broad bands with full width at half-maximum values $>1000 \text{ cm}^{-1}$ of f-d or charge transfer type in the UV-visible-near-infrared range.⁷⁹⁻⁸³ The broad bands of the two latter types of transitions are caused by considerably different equilibrium distances of ground and excited configuration, respectively, giving rise to vibronic transitions. Usually, the envelope of these vibronic transitions are observed, leading to broad bands,^{79,80} but in rare cases the

- (67) Amberger, H.-D.; Schultze, H.; Edelstein, N. M. *Spectrochim. Acta* **1986**, *42A*, 657.
 (68) Amberger, H.-D.; Reddmann, H.; Karsch, H. H.; Graf, V. W.; Qian, C.; Wang, B. *J. Organomet. Chem.* **2003**, *677*, 35.
 (69) Hayes, R. G.; Edelstein, N. M. *J. Am. Chem. Soc.* **1972**, *94*, 8688.
 (70) Edelstein, N. M. Organometallics of the f Elements. In *Electronic Structure of f Block Compounds*; Marks, T.; Fischer, R. D., Eds.; D. Reidel Publishing Company: Dordrecht, Holland, 1979.
 (71) Jank, S.; Amberger, H.-D. *Acta Phys. Pol.* **1996**, *A 90*, 21.
 (72) Jank, S.; Reddmann, H.; Amberger, H.-D. *Mat. Sci. For.* **1999**, *315-317*, 457.
 (73) Hazin, P. N.; Bruno, J. W.; Brittain, H.-G. *Organometallics* **1987**, *6*, 913; and references therein.
 (74) Reddmann, H.; Schultze, H.; Amberger, H.-D.; Apostolidis, C.; Kanellakopoulos, B. *Spectrochim. Acta* **1990**, *46A*, 1223.
 (75) Amberger, H.-D.; Reddmann, H.; Schultze, H.; Jank, S.; Kanellakopoulos, B.; Apostolidis, C. *Spectrochim. Acta Part A* **2003**, *59*, 2527; and references therein.
 (76) Amberger, H.-D.; Reddmann, H.; Edelmann, F. T. *J. Organomet. Chem.* **2005**, *690*, 2238.
 (77) Amberger, H.-D.; Reddmann, H. *Z. Anorg. Allg. Chem.* **2008**, *634*, 173.
 (78) Amberger, H.-D.; Rosenbauer, G. G.; Fischer, R. D. *Mol. Phys.* **1976**, *32*, 1291.
 (79) Blasse, G.; Brill, A. *J. Chem. Phys.* **1967**, *47*, 5139.
 (80) Rambaldi, P.; Monkonge, R.; Wolf, J. P.; Pedrini, C.; Gesland, J. Y. *Opt. Commun.* **1998**, *146*, 163.
 (81) Aull, B. F.; Jenssen, H. P. *Phys. Rev. B* **1986**, *34*, 6647.
 (82) Combes, C. M.; Dorenbos, P.; van Eijk, C. W. E.; Pedrini, C.; den Hartog, H. W.; Gesland, J. Y.; Rodnyi, P. A. *J. Lumin.* **1997**, *71*, 65.
 (83) Blasse, G. *Prog. Solid State Chem.* **1988**, *18*, 79; and references therein.

(62) Jørgensen, C. K. *Modern Aspects of Ligand Field Theory*; North-Holland Publishing Company: Amsterdam, 1971; p 306.

(63) Jørgensen, C. K. *Prog. Inorg. Chem.* **1962**, *4*, 73.

(64) Tandon, S. P.; Mehta, P. C. *J. Chem. Phys.* **1970**, *52*, 5417.

(65) Lang, R. J. *Can. J. Res.* **1936**, *14*, 122.

(66) Crosswhite, H. M.; Crosswhite, H. *J. Opt. Soc. Am.* **1984**, *B1*, 246.

vibronic structure can be resolved.⁸⁴ Characteristic for the luminescence spectra of Ce^{III} compounds is a (sometimes not resolved) couple of transitions which is presumed to result from transitions initiating at the lowest CF level of the term ²D and terminating on the multiplets ²F_{5/2} and ²F_{7/2}.⁷⁹ These d-f transitions range from approximately 50000 cm⁻¹ in the gaseous free Ce³⁺ ion⁸⁵ via 31250/29240 cm⁻¹ in [Ce³⁺·C₂.2.1.]Cl₃·2H₂O⁸⁶ and 14400/12580 cm⁻¹ in LaLuS₃:Ce³⁺^{87,88} to 13310/11920 cm⁻¹ in [Li(THF)₄]-[Ce(COT)₂]⁷⁶ (cf. Supporting Information, Table SI-3).^{89–93} This decrease is thought to reflect a lowering of the energy of the lowest d level brought on by the combined strong CF splitting and weaker spin-orbit coupling interactions within the set of five d orbitals (cf. eq 10).^{88,89} The difference of energies of the absorption transition initiating at ²F_{5/2} and terminating at the lowest CF level arising from ²D and the corresponding inverse luminescence transition is defined as a Stokes shift,^{79,81} and the mean value of the energies of both bands indicates roughly the zero phonon transition.⁷⁹

In contrast to Cp₃Ce(THF),⁷⁴ Cp₃Ce(NCMe)₂,⁷⁵ and Ce(C₅Me₄H)₃,⁷⁷ compound **5** exhibits no signals of f-f origin in the FIR/IR and Raman spectra, neither at room nor at low temperatures. However, in the UV-visible range of the absorption spectrum, a distinctive broad band of f-d or charge-transfer type appeared at approximately 18750 cm⁻¹, and some diffuse shoulders superimposed on a broad ascent in the absorbance could be detected. In the excitation spectrum (monitoring the emission wavelength at 572 nm, corresponding to 17482 cm⁻¹) one sharp signal at 35030 cm⁻¹ and two broad asymmetric bands with maxima at approximately 24780 cm⁻¹ and 18800 cm⁻¹ appeared (Supporting Information, Figure SI-1). Monitoring the emission wavelength at 465 nm (21500 cm⁻¹) the former broadband could be resolved into a signal with a maximum at 24750 cm⁻¹ and a shoulder at 28090 cm⁻¹. Using the exciting lines at 458 and 514.5 nm of an Ar⁺ laser, two extremely strong and broad asymmetric luminescence bands with maxima at about 17550 cm⁻¹ and 16150 cm⁻¹ appeared. Applying the exciting lines at 404 and 320 nm, respectively, additional broad, partly structured bands at approximately 21500 cm⁻¹, 23600 cm⁻¹, and 27700 cm⁻¹ could be observed. At 77 K, some weak shoulders appeared on the low energetic side of the broad bands with maxima at about 17550 cm⁻¹ and 16150 cm⁻¹.

According to the results of a (DV)-X α calculation of Kaltsoyannis and Bursten⁹⁴ the lowest 6d level of the 5f¹ system Pa(COT)₂ is of d_σ (d_{z²}) type. Adopting these results, the couple of broad bands at 17550 cm⁻¹ and 16150 cm⁻¹ of compound **5** are due to transitions initiating at 5d_σ and terminating at the multiplets ²F_{5/2} and ²F_{7/2}, respectively. With the exception of [Li(THF)₄][Ce(COT)₂], the above-mentioned values are lower than all luminescence energies ever communicated before for organometallic Ce^{III} compounds (Supporting Information, Table SI-3). This indicates that the combined interactions of the COT and Tp^{Me2} ligands with the set of d orbitals is extremely strong (cf. eq 10). To examine which one of the two ligands causes the main contribution, we also recorded the luminescence spectrum of Ce(Tp)₃. This compound exhibits a broad unresolved band with a maximum at approximately 18900 cm⁻¹ and [Li(THF)₄][Ce(COT)₂] a couple of signals at 13310 and 11920 cm⁻¹ (Supporting Information, Figure SI-1, Table SI-3). These findings demonstrate that the energetic lowering of 5d_{z²} → ²F_{7/2}/²F_{5/2} transitions for compound **5** is mainly due to the strong interaction of 5d_{z²} with the COT, and not the Tp^{Me2} ligand. In contrast to these experimental results for compound **5** and [Li(THF)₄][Ce(COT)₂], the above-mentioned model calculation for Pa(COT)₂ predicts only a weak, predominantly non-bonding interaction between the 6d_{z²} orbital and the corresponding symmetry-adapted linear combination of the carbon p_z orbitals of the COT ligand.⁹⁴ The Stokes shift of compound **5** is with about 1200 cm⁻¹ noticeably lower than in LiYF₄:Ce³⁺ (2000 cm⁻¹)⁸¹ or in Rb₂NaYF₆:Ce³⁺ (7000 cm⁻¹).⁸⁰ The energies of the absorption transition ²F_{5/2} → dσ (18750 cm⁻¹) and the inverse luminescence transition (17550 cm⁻¹) suggest that the zero-phonon line is approximately at 18150 cm⁻¹. This value is even lower than the very low values of Y₂O₂S:Ce³⁺ (19000 cm⁻¹)⁸⁰ or Lu₂O₂S:Ce³⁺ (19300 cm⁻¹).⁹⁰

The absorption bands in the UV-visible range (as well as the corresponding signals in the excitation spectra) of colorless Ce^{III} compounds such as [Ce(H₂O)₉]³⁺ or LiYF₄:Ce³⁺ are interpreted in terms of transitions terminating on d levels caused by combined CF and spin-orbit coupling effects.^{81,82,89} Ce^{III} organometallics, however, are frequently deeply colored, suggesting possible charge-transfer transitions. No help with the assignment of the signals observed in the excitation spectra of **5** may be expected from quantum chemistry, as results of model calculations on the 4f¹ systems **5**, [Ce(COT)]⁺, and [K(diglyme)][Ce(COT)₂] have not been communicated up to now. However, the 4f¹ system Ce(COT)₂⁹⁵ and the 5f¹ system Pa(COT)₂⁹⁴ were targets of a number of model calculations of different degrees of sophistication. For both compounds, low lying predominantly ligand-based levels were predicted; thus, the signals in the

(84) Szcurek, T.; Schlesinger, M. In *Rare Earth Spectroscopy*; Jezowska-Trzebiatowska, B., Legendziewicz, J., Streck, W., Eds.; World Scientific: Singapore, 1985; p 309.

(85) Brewer, L. *J. Opt. Soc. Am.* **1971**, *61*, 1666.

(86) Blasse, G.; Dirksen, G. J.; Sabatini, N.; Peradhone, S. *Inorg. Chim. Acta* **1987**, *133*, 167.

(87) Scharmer, E.-G. Dissertation, Hamburg, 1982.

(88) Dorenbos, P. *Mat. Sci. For.* **1999**, *315–317*, 222; and references therein.

(89) Okada, K.; Kaizu, J.; Kobayashi, H.; Tanaka, K.; Marumoto, F. *Mol. Phys.* **1985**, *54*, 1293.

(90) Yokono, S.; Abe, T.; Hoshina, T. *J. Lumin.* **1981**, *24/25*, 309.

(91) Amberger, H.-D.; Edelmann, F. T.; Apostolidis, C.; unpublished results.

(92) Jank, S. Dissertation, Hamburg 1998.

(93) van't Spijker, J. C.; Dorenbos, P.; van Eijk, C. W. E.; Güdel, H. U.; Krämer, K. *J. Lumin.* **1999**, *85*, 1.

(94) Kaltsoyannis, N.; Bursten, B. E. *J. Organomet. Chem.* **1997**, *528*, 19; and references therein.

(95) Dolg, M.; Stoll, H. In *Electronic Structure Calculations for Molecules Containing Lanthanide Atoms*; Gschneidner, K. A., Jr.; Eyring, L., Eds.; Handbook on the Physics and Chemistry of Rare Earths; Elsevier Science B.V.: Amsterdam, 1996; Vol. 22, Chapter 152, and references therein.

excitation spectrum of compound **5** may be partly of charge-transfer type.

Jørgensen et al. applied eq 10 to the f-f transitions of LnCp₃ (Ln = Pr, Nd, Er)⁹⁶ and Nugent et al. to those of AnCp₃ (An = Am, Cm),⁹⁷ ending up with covalent characters between 2.8 and 5.5% for the f-type wave functions. Hazin et al., however, applied this relation to the above-mentioned couple of d-f luminescence transitions⁷³ (making use of the luminescence bands at 31950 and 30000 cm⁻¹ of [Ce(H₂O)₉]³⁺)⁸⁹ of a number of Ce^{III} organometallics (cf. Supporting Information, Table 3) and found covalencies between 6% and 22%. The energy of emission E_{em} from the lowest energy 5d¹f⁰ configuration level to the ground multiplet ²F_{5/2} can be expressed as⁸⁸

$$E_{em} = E_{free} - \Delta E_{bc} - \Delta E_{cfs} - \Delta E_s \quad (11)$$

where E_{free} is the emission energy of the gaseous free Ce³⁺ ion, ΔE_{bc} is the energy difference between E_{free} and the barycenter energy of the d terms arising from the 5d¹f⁰ configuration of the compound of interest. ΔE_{cfs} is the energy difference between the lowest 5d¹f⁰ level and the barycenter energy of the d terms caused by CF splitting effects, and ΔE_s is the Stokes shift between absorption and emission.⁸⁸ This means that the energies of the observed couple of luminescence transitions mainly reflect the CF splitting effects of excited 5d orbitals of Ce^{III} compounds and not exclusively covalency effects of d or f type wave functions, and thus the covalency data given for f orbitals by Hazin et al.⁷³ are suspect.

(b) (COT)Pr[Tp^{Me2}] (6). In ref 40 the optical and magnetochemical properties of powdered scorpionate **6** have been studied and interpreted on the basis of phenomenological CF theory. For this reason, only the procedure and the more important results are summarized here. In the low temperature absorption spectrum (ca. 30 K), transitions initiating at the (somewhat split) ground state $|\pm 3\rangle$ and terminating at the CF states of the multiplets ³F_{2,3,4}, ¹G₄, ¹D₂, ³P₀, ³P₁, ¹I₆, and ³P₂ could be observed. Since, at that time, the experimental separation of “cold” and “hot” transitions was not certain in all cases, we repeated these measurements using a bath cryostat equipped with liquid He which allowed the recording of satisfactorily resolved spectra in the gas phase between 5 and 15 K. The accumulated new data (Supporting Information, Figure SI-2) confirmed the previous assignments in all cases. The luminescence spectrum is dominated by the transitions ³P₀ → ³H_{4,5,6}, ³F_{2,3,4}. Because of the perturbing field of the Tp^{Me2} ligand, numerous CF states which are 2-fold degenerate in C_{∞v} symmetry are split into two components with energy separations of 20–43 cm⁻¹. As mentioned before, the initial state of the low temperature absorption transitions is roughly described by $|\pm 3\rangle$, that of the luminescence transitions by $|0\rangle$, and transitions to the terminal levels ³F_{2,3,4} are observed in both types of spectra. Assuming that the selection rules for C_{∞v} symmetry hold

roughly for compound **6**, several (partly split) CF levels could be identified. Fitting the free parameters of the phenomenological Hamiltonian (eq 4) to the experimental CF energies of these levels, a preliminary set of free ion and CF parameters could be derived. A number of still unidentified experimental CF levels were close to the eigenvalues of the preliminary fit and were identified with the wave functions of these eigenvalues. The free parameters of two somewhat different Hamiltonians were fitted to the energies of both the calculational and the previously experimentally assigned CF levels. In the first fit C_{∞v} symmetry of the effective CF was assumed, and the energetic barycenters of split CF levels were fitted. In the second, the observed splitting of degenerate levels (in C_{∞v} symmetry) was considered by introducing the perturbing parameter B₆⁰. The first fit is representative for the cationic model compound [Pr(COT)]⁺, and the second for the real scorpionate **6**. The parameter sets used in the fits, as well as the values of σ and $N_f/\sqrt{4\pi}$ for both compounds, are given in Supporting Information, Table SI-4. Thus, the obtained CF parameters for [Pr(COT)]⁺ are considered as a master parameter set for the interpretation of the optical spectra of other (COT)Ln(scorpionates). On the basis of the wave functions and eigenvalues of the latter fit, but using the experimental CF energies of the ground multiplet ³H₄, the temperature dependence of μ_{eff}^2 was calculated and is seen to be in excellent agreement with the experimental value (Supporting Information, Figure SI-3a).

For comparison purposes with the 5f² system [U^{IV}(COT)]²⁺ (vide infra), the found energy sequence of CF levels of the ground multiplet ³H₄ of [Pr(COT)]⁺ is also given here:

$$E(|\pm 3\rangle) < E(|\pm 2\rangle) \ll E(|\pm 1\rangle) < E(|\pm 4\rangle) < E(|0\rangle)$$

(c) (COT)Pr[Tp] (2). Scorpionate **2** exhibits nicely resolved absorption spectra in solution, but up to now, we obtained only less satisfactorily resolved spectra from pellets. Luminescence spectra, however, could only be observed using polycrystalline material (vide infra). At room temperature, the absorption transitions of f-f character in the range > 19000 cm⁻¹ are superimposed on the ascending slope of a broad intense f-d or charge-transfer band with a maximum at approximately 29500 cm⁻¹. However, at low temperatures this broad band is shifted to higher energies, and the f-f signals in this range can be observed without any difficulties. Besides, numerous “hot” bands with energy separations of about 180, 680, 780, and 860 cm⁻¹ from the corresponding “cold” bands disappeared. At room temperature, several groups of more or less broad luminescence signals appeared, which have to be correlated, in analogy with the corresponding bands of compound **6**, with transitions initiating at ³P₀ and terminating at CF levels of ³H_{4,6} and ³F_{2,3,4}, respectively. An additional group of positive and negative signals could be observed between 17000 and 16000 cm⁻¹. The positive peaks in this range are usually due to the luminescence transition ¹D₂ → ³H₄, and the negative ones arise from absorption of background radiation of the inverse absorption transition ³H₄ → ¹D₂.⁴⁰

(96) Jørgensen, C. K.; Pappalardo, R.; Flahaut, J. *J. Chim. Phys.* **1965**, *62*, 444.

(97) Nugent, L. J.; Laubereau, P. G.; Werner, G. K.; vander Sluis, K. L. *J. Organomet. Chem.* **1971**, *27*, 365.

Cooling down to approximately 100 K, two additional negative signals appeared at 20264 and 20293 cm^{-1} , which have to be associated with the transition from $^3\text{P}_0$ to the obviously somewhat split CF ground state $|\pm 3\rangle$. Besides, the broader bands of transitions $^3\text{P}_0 \rightarrow ^3\text{H}_{4,6}$, $^3\text{F}_{2,3,4}$ in the room temperature luminescence spectrum split partly into two components, and the positive signal at 16130 cm^{-1} changed sign and split into two components at 16154 and 16112 cm^{-1} . The absorption transition from the ground state $|\pm 3\rangle$ to $^3\text{P}_0$ corresponds in (glassy frozen) methylcyclohexane/toluene solution to one single peak which moves from 20196 cm^{-1} at room temperature via 20211 cm^{-1} at about 90 K to 20213 cm^{-1} at about 30 K. Powdered material, however, exhibits at approximately 100 K two signals at 20264 and 20293 cm^{-1} in the luminescence spectrum. The splitting indicates that the 2-fold degeneracy of the CF ground state $|\pm 3\rangle$ in solution is lifted by the perturbing field of the $[\text{Tp}]^-$ ligand, and the observed shift between solution and powder data demonstrate that even inert solvents cause solvation effects. Of course, this effect shifts also the CF energies of other states, and the descent in symmetry (in the solid state) also splits the CF levels of degenerate states; thus, the CF splitting patterns derived from solution absorption and luminescence spectra of powdered material differ somewhat. As the former set of data is more complete, we focus here on the CF splitting pattern of compound **2** extracted from solution absorption spectra. By comparing the 90 K absorption spectrum of dissolved compound **2** with those of powdered scorpionate **6** recorded at approximately 90 K and between 5–15 K, respectively (Supporting Information, Figure SI-2), the “cold” transitions of **2** could be separated from the “hot” ones. Fitting the free parameters of the phenomenological Hamiltonian (eq 4) to the experimental CF energies, a σ value of 28.4 cm^{-1} (for 18 assignments) could be achieved. The complete set of parameters along with the value of $N_i/\sqrt{4\pi}$ is given in Supporting Information, Table SI-4.

(d) (COT)Nd[Tp^{Me2}] (7). In ref 41 we reported on the absorption spectrum of compound **7** dissolved in a mixture of methylcyclohexane/toluene (of the ratio 2:1) run at ambient temperature, at 90 K, and partly at approximately 30 K. Because of a limited supply of liquid He, only transitions to excited multiplets with lower J values were measured using this coolant. The CF splitting pattern of the ground manifold $^4\text{I}_{9/2}$ was extracted from the “hot” transition $^4\text{I}_{9/2} \rightarrow ^2\text{P}_{1/2}$ and those of the analyzed excited multiplets from the 90 and 30 K absorption spectra, respectively. Making use of the free ion parameters of $\text{Cp}_3\text{Nd}(\text{MeTHF})$ and the CF parameters of $[\text{Pr}(\text{COT})]^+$, the observed absorption signals of scorpionate **7** were identified on the basis of the calculational method.^{56–58} In a subsequent fitting procedure, the free ion parameters F^2 , F^4 , F^6 , and ζ_{4f} as well as the CF parameters B_0^2 , B_0^4 , B_0^6 were fitted to the energies of 27 levels, leading to the final values as given in Supporting Information, Table SI-4. To check the goodness of the fit, the temperature dependence of μ_{eff}^2 was calculated on the basis of the wave functions and eigenvalues of the fit; the experimental energies were used only in case of the ground multiplet. Introducing

an orbital reduction factor,⁹⁸ $k = 0.965$, experimental and calculated values agree in a satisfactory manner (Supporting Information, Figure SI-3b).⁴¹ The energetic sequence of CF levels on the ground multiplet $^4\text{I}_{9/2}$ is as follows: $E(|\pm 5/2\rangle) < E(|\pm 7/2\rangle) < E(|\pm 3/2\rangle) \ll E(|\pm 9/2\rangle) < E(|1/2\rangle)$. The CF ground state $|\pm 5/2\rangle$ of the $4f^3$ system **7** agrees with that of the $5f^3$ system $\text{Np}^{\text{IV}}(\text{COT})_2$ concluded from susceptibility and NMR data.^{99–101}

(e) (COT)Sm[Tp] (4). The optical properties of scorpionate **4** have been studied by means of glassy frozen solutions, KBr pellets, and single crystals of the size $2.5 \times 1 \times 1$ mm.⁹² Because of a low-lying charge-transfer transition, signals of f-f character in the absorption spectrum could only be observed in the range below 18000 cm^{-1} . Unfortunately, the deep red color of compound **4** prevents the observation of a well-resolved luminescence spectrum, on the basis of which the CF splitting patterns of organometallic Sm^{III} compounds in the low energetic range are usually derived.⁵⁷ In spite of the small size of the single crystal, its unpolarized room temperature absorption spectrum was of comparable quality as that of the corresponding solution and better than that of the pellet (Supporting Information, Figure SI-4). A number of different orientations of the orthorhombic single crystal and polarizers were applied, but only weak polarization effects could be observed in absorption (and no in emission), which do not allow the experimental assignment of observed transitions. The main reason for this is that the axes (defined by the barycenters of the COT ring and the three coordinating N atoms of the Tp ligand) of the two pairs of molecules in the unit cell are not aligned but enclose angles of approximately 30° (value for Pr). Therefore, again a calculational^{56–58} and not an experimental identification procedure had to be applied. The free parameters of a phenomenological Hamiltonian (eq 4) were fitted to the thus identified levels. The final parameter set, as well as the corresponding $N_i/\sqrt{4\pi}$ and σ values, are given in Supporting Information, Table SI-4.

Because of the strong field dependence of the experimental susceptibility, the accuracy of the fit could not be checked by comparing calculated and experimental magnetic data.

(f) (COT)Sm[Tp^{Me2}] (8). Because of a low-lying charge-transfer transition of violet scorpionate **8**, signals of f-f character could not be observed in the luminescence spectrum, and in the absorption spectrum (methylcyclohexane/toluene solution) only between 6050–10850 cm^{-1} . The absorption spectra of compounds **8** and **4** exhibit in the NIR range essentially the same features (Supporting Information, Figure SI-4), but the total CF splitting of the multiplet $^6\text{F}_{11/2}$

(98) Stevens, K. W. H. *Proc. Roy. Soc. (London)* **1954**, A219, 542.

(99) Karraker, D. G.; Stone, J. A.; Jones, E. R., Jr.; Edelstein, N. M. *J. Am. Chem. Soc.* **1970**, 92, 4841.

(100) Bolander, R. Dissertation, University of Karlsruhe, Karlsruhe, Germany, 1983.

(101) Klenze, R. Dissertation, University of Heidelberg, Heidelberg, Germany, 1985.

(in the vicinity of the above-mentioned charge-transfer band) is noticeably stronger for **8** (620 cm^{-1}) than for **4** (500 cm^{-1}).

(g) (COT)Er[Tp] (**9**). Er^{III} compounds frequently exhibit luminescence transitions, on the basis of which the energies of lower lying CF levels can be extracted (see ref 52, p 294). Using the exciting lines at 458 and 488 nm of an Ar⁺ laser, only “negative” peaks could be observed instead of the expected “positive” ones. The reason for this finding is that compound **9** contains traces of an organic dye which exhibits broadband fluorescence (comparable to a continuous light source). This broadband fluorescence initiates transitions from CF states thermally populated at the temperatures of measurements to higher CF states and is thus partly absorbed, leading to an absorption instead of the expected luminescence spectrum (Supporting Information, Figure SI-5). The “ordinary” absorption spectrum of a KBr pellet exhibits comparable features at room temperature, but the absorption spectrum from broadband luminescence is noticeably better resolved in the range of the transition $^4\text{I}_{15/2} \rightarrow ^4\text{S}_{3/2}$. Immersing the pellet in liquid N₂, the above-mentioned group of transitions corresponds to two “cold” signals at 18195 and 18320 cm^{-1} which are accompanied by “hot” transitions initiating at excited CF levels separated approximately 130 and 230 cm^{-1} from the CF ground state (Supporting Information, Figure SI-5). Inserting the CF parameters of compound **6** and the free ion parameters of Er[CH-(SiMe₃)₂]₃¹⁰² the CF states of $^4\text{S}_{3/2}$ are predicted at 18240 and 18305 cm^{-1} , which is comparable with the experimental finding. Assuming C_{∞v} symmetry, the ground multiplet $^4\text{I}_{15/2}$ of compound **9** leads to eight CF levels which are partly thermally populated at about 80 K. For this reason, a successful CF analysis is impossible on the basis of the currently available 80 K absorption spectrum. Additionally, this analysis is rendered more difficult by vibronic coupling of skeletal and innerligand vibrations. Low temperature measurements using liquid He as coolant are in progress.

(COT)UI₂(THF)₂. From the findings that scorpionate **7** and (COT)NdI(THF)₃ have nearly identical absorption spectra³⁹ and that the CF strengths experienced by the Ln³⁺ central ions of Ln(Tp)₃ (Ln = Pr, Nd, Sm) are not too strong,^{42,122,132} we concluded that the CF effects of the two former compounds are essentially produced by the [Ln(COT)]⁺ moiety (vide supra). It is tempting to assume that the CF effects of (COT)UI₂(THF)₂ are also essentially due to the [U(COT)]²⁺ moiety and that the CF parameters of [U(COT)]²⁺ are comparable with those of [Pr(COT)]⁺ apart from a scaling factor of 3–4. This scaling factor considers the finding that the CF strengths of U^{IV} compounds are by a factor of 3–4 larger than those of the corresponding Pr^{III} compounds (for example, cf. Supporting Information, Table SI-5).^{105–117}

The tentative diagonalization of the energy matrix of an f² system into which the CF parameters of [Pr(COT)]⁺, multiplied by three, and the free ion parameters of Cp₃UCl¹⁰³ have been inserted, yields eigenvalues which are comparable with the band maxima of a number of transitions in the absorption spectrum of (COT)UI₂(THF)₂. A subsequent fitting procedure led to the parameter set as given in Supporting Information, Table SI-4.¹⁰⁴ Surely, this ad hoc procedure has no serious scientific justification, but Supporting Information, Figure SI-6 and Table SI-8 show that the doubled CF parameters of (COT)UI₂(THF)₂ are comparable to those of more recent model calculations on U(COT)₂ and Pa(COT)₂. Besides, the CF levels of the ground multiplet ³H₄ have the same energetic sequence E(|±3⟩) < E(|±2⟩) < E(|0⟩) < E(|±1⟩) < E(|±4⟩) predicted for U(COT)₂ in recent years (vide infra).

2.5. Spectrochemical and Nephelauxetic Effects of (COT)Ln(scorpionates). In Supporting Information, Tables SI-5, SI-6, and SI-7,^{118–135} the global CF strengths $N_i/\sqrt{4\pi}$ experienced by the Ln³⁺ central ions of complexes **2**, **4**, **6**, and **7** are compared with those of other molecular Ln^{III} compounds and some representative Ln^{III} salts and solids. It can be seen from these tables that the highest global CF strengths are found for Ln(C₃Me₄H)₃ and the *t*-Bu- and SiMe₃-substituted LnCp'₃ (Ln = Pr, Nd, Sm) compounds.

In Supporting Information, Table SI-5, the values of the nephelauxetic parameters beta_F, beta_E, beta_J and the relativistic nephelauxetic parameters beta' of compounds **2** and **6** are compared with those of other Pr^{III} compounds. The ordering of beta_F, beta_E, beta_J, and beta' values does not coincide in most cases but typically beta_F < beta_E < beta_J < beta'. The difference between beta_E and beta_J lies around 2%. The reason for this is that the covalency of [Ln(H₂O)₉]⁺ is not completely negligible, as already suggested by Nugent et al.⁹⁷ Inserting the beta_F, beta_E, and beta_J values of compounds **2** and **6**, respectively (see Supporting Information, Table SI-5) into relation 9, one ends up with covalency degrees between 18–20%. In Supporting Information, Tables SI-6 and SI-7, the F², ζ_{4f}, and $N_i/\sqrt{4\pi}$ values of scorpionates

- (102) Reddmann, H.; Guttenberger, C.; Amberger, H.-D. *J. Organomet. Chem.* **2000**, *602*, 65.
(103) Amberger, H.-D.; Reddmann, H.; Edelstein, N. M. *Inorg. Chim. Acta* **1988**, *141*, 313.
(104) Jank, S.; Reddmann, H.; Amberger, H.-D.; Ephritikhine, M.; Berthet, J.-C. *XIII FECEM*, Conference on Organometallic Chemistry, 1999, August 29th-September 3rd, Lisbon, Portugal, Poster P9.

- (105) Jayasankar, C. K.; Reid, M. F.; Richardson, F. S. *Phys. Status Solidi B* **1989**, *155*, 559.
(106) Richardson, F. S.; Reid, M. F.; Dallara, J. J.; Smith, R. B. *J. Chem. Phys.* **1985**, *83*, 3813.
(107) Hagen, C.; Reddmann, H.; Amberger, H.-D.; Edelmann, F. T.; Pegelow, U.; Shalimoff, G. V.; Edelstein, N. M. *J. Organomet. Chem.* **1993**, *462*, 69.
(108) Amberger, H.-D.; Jank, S.; Reddmann, H.; Edelstein, N. M. *Spectrochim. Acta Part A* **2002**, *58*, 379.
(109) Jank, S.; Reddmann, H.; Amberger, H.-D. *J. Alloys Compd.* **1997**, *250*, 387.
(110) Amberger, H.-D.; Schultze, H.; Edelstein, N. M. *Spectrochim. Acta* **1985**, *41A*, 713.
(111) Reddmann, H.; Schultze, H.; Amberger, H.-D. *Eur. J. Solid State Inorg. Chem.* **1991**, *28*, 69.
(112) Unrecht, B.; Reddmann, H.; Amberger, H.-D. *J. Alloys Compd.* **1998**, *275–277*, 323.
(113) Apostolidis, C.; Kanellakopoulos, B.; Klenze, R.; Reddmann, H.; Schulz, H.; Amberger, H.-D. *J. Organomet. Chem.* **1992**, *426*, 307.
(114) Amberger, H.-D.; Reddmann, H., in preparation.
(115) Amberger, H.-D.; Yünlü, K.; Edelstein, N. M. *Spectrochim. Acta* **1986**, *42A*, 27.
(116) Satten, R. A.; Schreiber, C. L.; Wong, Y. *J. Chem. Phys.* **1963**, *42*, 162.
(117) von Deurzen, C. H. H.; Rajnak, K.; Conway, J. G. *J. Opt. Soc. Am.* **1984**, *1*, 45.

7 and 4 (F^2 and ζ_{4f} of gaseous Nd^{3+} and Sm^{3+} are not known) are compared to those of other Nd^{III} and Sm^{III} compounds, respectively. Like in the case of Pr^{III} compounds, the ordering of F^2 values does not coincide with those of ζ_{4f} values.

2.6. Experimentally Based and Calculated MO Schemes (in the f Range) of COT Complexes of f Elements. Up to now, the $[\text{Ln}(\text{COT})]^+$ and $[\text{U}(\text{COT})]^{2+}$ moieties were not targets of quantum chemical model calculations, but the results of a MHW-MO calculation on $[\text{Ln}(\text{COT})_2]^{-136}$ and of a number of model calculations of very different degrees of sophistication on $\text{An}^{\text{IV}}(\text{COT})_2$ ($\text{An} = \text{Th}, \text{Pa}, \text{U}, \text{Np}, \text{Pu}$) have been communicated.^{69,94,136–145} The CF parameters of $[\text{Ln}(\text{COT})_2]^-$ are assumed to be approximately twice as large as those of $[\text{Ln}(\text{COT})]^+$, and the CF strengths of several U^{IV} compounds are approximately three to four times as large as those of the corresponding Pr^{III} analogues (cf. for example, $\text{Cs}_2\text{NaPrCl}_6$ and Cs_2UCl_6 or $(\text{NEt}_4)_2\text{UCl}_6$ in Supporting Information, Table SI-5). For this reason, in Figure 4, when comparing the experimentally oriented non-relativistic MO schemes of $[\text{Pr}(\text{COT})]^+$ and $[\text{U}(\text{COT})]^{2+}$ with the calculated ones of $\text{U}(\text{COT})_2$ (MRCISD calculation,¹⁴³ fitted by CF and free ion parameters)¹⁰⁴ and

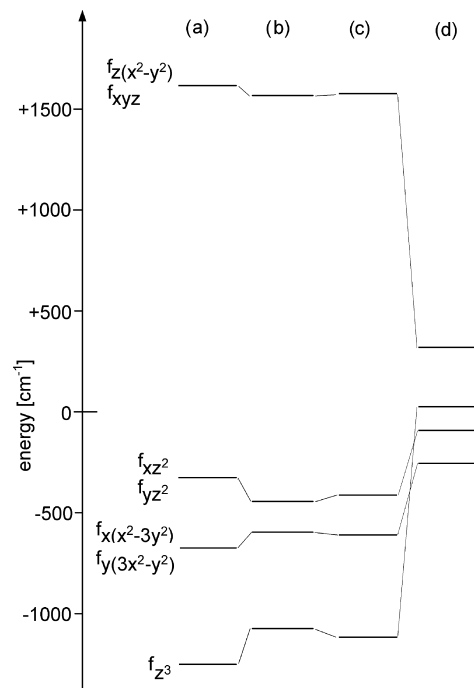


Figure 4. Comparison of non-relativistic MO schemes in the f range: (a) $[\text{Pr}(\text{COT})]^+$, experimentally based; (b) $[\text{U}(\text{COT})]^{2+}$, experimentally based; (c) $\text{U}(\text{COT})_2$, calculated, fitted data of ref 143; (d) $[\text{Ln}(\text{COT})_2]^-$, calculated (ref 136). For purposes of better comparison, the orbital energies of the above-mentioned compounds have been multiplied by 2, 2/3, 1/3, and 1, respectively (see text for details).

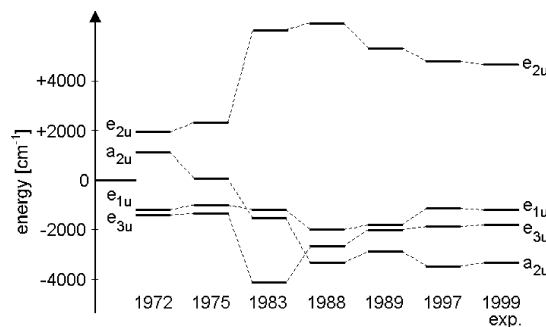


Figure 5. Comparison of selected previously computed f orbital energies of $\text{U}(\text{COT})_2$. Used references: 1972,⁶⁹ 1975,¹³⁶ 1983,¹³⁸ 1988,¹³⁹ 1989,¹⁴⁰ 1997,¹⁴³ 1999¹⁰⁴ (exp.: doubled values of $[\text{U}(\text{COT})]^{2+}$).

$[\text{Ln}(\text{COT})_2]^-$,¹³⁶ the energies of the first two compounds were multiplied by two, and additionally all values for the U^{IV} compounds divided by three. As can be seen from Figure 4, not only the energetic sequence but also the total splitting of f orbitals is comparable for the above specified situations for $[\text{Pr}(\text{COT})]^+$, $[\text{U}(\text{COT})]^{2+}$, and $\text{U}(\text{COT})_2$ but not for $[\text{Ln}(\text{COT})_2]^-$.

In Figure 5, the f orbital energies (referred to the energetic barycenter of f orbitals) of some representative non-relativistic and fitted relativistic model calculations on $\text{U}(\text{COT})_2$ are given. It is very remarkable that the more recent calculations produce the energetic sequence $E(a_{2u}) < E(e_{3u}) < E(e_{1u}) < E(e_{2u})$ (Figure 5) which is compatible with the experimentally oriented non-relativistic sequence of f orbitals for $[\text{Pr}(\text{COT})]^+$ and the tentative one for $[\text{U}(\text{COT})]^{2+}$ (Figure 4). In Supporting Information, Table SI-8, the CF parameters extracted from a number of calculated orbital energies for $[\text{Ce}(\text{COT})_2]^-$, $\text{Pa}(\text{COT})_2$, and $\text{U}(\text{COT})_2$ are summarized.

- (118) Reddmann, H.; Apostolidis, C.; Walter, O.; Amberger, H.-D. *Z. Anorg. Allg. Chem.* **2006**, 632, 1405.
- (119) Reddmann, H.; Amberger, H.-D.; Kanellakopoulos, B.; Maiwald, S.; Taube, R. *J. Organomet. Chem.* **1999**, 584, 310.
- (120) Amberger, H.-D.; Reddmann, H.; Unrecht, B.; Edelmann, F. T.; Edelstein, N. M. *J. Organomet. Chem.* **1998**, 566, 125.
- (121) Jank, S.; Hanss, J.; Reddmann, H.; Amberger, H.-D.; Edelstein, N. M. *Z. Anorg. Allg. Chem.* **2002**, 628, 1355.
- (122) Jank, S.; Amberger, H.-D.; Edelstein, N. M. *Spectrochim. Acta Part A* **1998**, 54, 1645.
- (123) Reddmann, H.; Schultze, H.; Amberger, H.-D.; Shalimoff, G. V.; Edelstein, N. M. *J. Organomet. Chem.* **1991**, 411, 331.
- (124) Amberger, H.-D.; Jank, S.; Reddmann, H.; Edelstein, N. M. *Mol. Phys.* **1997**, 90, 1013.
- (125) Jank, S.; Reddmann, H.; Amberger, H.-D.; Apostolidis, C. *J. Organomet. Chem.* **2004**, 689, 3143.
- (126) Amberger, H.-D.; Reddmann, H. *Z. Anorg. Allg. Chem.* **2007**, 633, 443.
- (127) Guttenberger, C.; Unrecht, B.; Reddmann, H.; Amberger, H.-D. *Inorg. Chim. Acta* **2003**, 348, 165.
- (128) May, S.; Reid, M. F.; Richardson, F. S. *Mol. Phys.* **1987**, 62, 341.
- (129) Reddmann, H.; Apostolidis, C.; Walter, O.; Rebizant, J.; Amberger, H.-D. *Z. Anorg. Allg. Chem.* **2005**, 631, 1487.
- (130) Hölsä, J.; Lamminmäki, R.-J. *J. Lumin.* **1996**, 69, 311–317.
- (131) Schulz, H.; Reddmann, H.; Amberger, H.-D. *J. Organomet. Chem.* **1993**, 461, 69.
- (132) Qian, C.; Wang, B.; Edelstein, N. M.; Reddmann, H.; Amberger, H.-D. *J. Alloys Compd.* **1994**, 207–208, 87.
- (133) Reddmann, H.; Jank, S.; Amberger, H.-D. *Spectrochim. Acta Part A* **1997**, 53, 495.
- (134) Amberger, H.-D.; Reddmann, H. *J. Organomet. Chem.* **2007**, 692, 5103.
- (135) Reddmann, H.; Amberger, H.-D.; Evans, W. J., in preparation.
- (136) Warren, K. D. *Inorg. Chem.* **1975**, 14, 3095.
- (137) Pyykkö, P.; Lohr, L. L. *Inorg. Chem.* **1981**, 20, 1950.
- (138) Rösch, N.; Streitwieser, A., Jr. *J. Am. Chem. Soc.* **1983**, 105, 7237.
- (139) Boerrigter, P. M.; Baerends, E. J.; Snijders, J. G. *Chem. Phys.* **1988**, 122, 357.
- (140) Chang, A. H.; Pitzer, R. M. *J. Am. Chem. Soc.* **1989**, 111, 2500.
- (141) Chang, A. H.; Ermiler, W. C.; Pitzer, R. M. *J. Alloys Compd.* **1994**, 213, 191.
- (142) Liu, W.; Dolg, M.; Fulde, P. *J. Chem. Phys.* **1997**, 107, 3584.
- (143) Dolg, M., personal communication, Oct 1997.
- (144) Li, J.; Bursten, B. E. *J. Am. Chem. Soc.* **1998**, 120, 11456.
- (145) Li, J.; Bursten, B. E. The Electronic Structure of Organoactinide Complexes via Relativistic Density Functional Theory: Applications to the Actinocene Complexes $\text{An}(\eta^8\text{-C}_8\text{H}_8)_2$ ($\text{An} = \text{Th-Am}$) In *Computational Organometallic Chemistry*; Cundari, T. R., Ed.; Marcel Dekker: New York, 2001; p 345.

Interestingly, the more accurate calculations lead to a dominant negative B_0^4 parameter. In the experimentally oriented relativistic MO schemes for $[\text{Pr}(\text{COT})]^+$ and $[\text{U}(\text{COT})]^{2+}$, the energetic sequence $E(|\pm 1/2\rangle) < E(|\pm 5/2\rangle) < E(|\pm 3/2\rangle) \ll E(|\pm 1/2\rangle) < E(|\pm 7/2\rangle) < E(|\pm 3/2\rangle) < E(|\pm 5/2\rangle)$ results, with total splittings of 3690 and 9280 cm^{-1} , respectively. This sequence does not agree with the calculated one for $\text{U}(\text{COT})_2$ (REX approximation) as given in ref 137: $E(|\pm 5/2\rangle) \leq E(|\pm 1/2\rangle) < E(|\pm 3/2\rangle) \ll E(|\pm 7/2\rangle) < E(|\pm 1/2\rangle) < E(|\pm 3/2\rangle) < E(|\pm 5/2\rangle)$ (total splitting of $\sim 6900 \text{ cm}^{-1}$).

In recent years, the CF splitting patterns of $\text{Pa}(\text{COT})_2$ and $\text{U}(\text{COT})_2$ were calculated on the basis of various relativistic approximations.^{139–145} This offers the unique chance to fit the free parameters of a phenomenological Hamiltonian to these calculated CF splitting patterns. Of course, this procedure yields only realistic free ion and CF parameters if covalency effects may be safely neglected (which does not hold strictly for An^{IV} organometallics),^{137–145} but we expect valuable hints on the signs and orders of magnitude of CF parameters. In case of the fits of the various calculated CF splitting patterns of $\text{Pa}(\text{COT})_2$ as given by Kaltsoyannis and Bursten,⁹⁴ Li and Bursten,^{144,145} and Chang et al.,¹⁴¹ respectively, and that of $\text{U}(\text{COT})_2$ communicated by Liu et al.¹⁴² and by Dolg,¹⁴³ the fits converged, but not in the case of the calculated CF splitting pattern of $\text{U}(\text{COT})_2$ given by Chang and Pitzer¹⁴⁰ (cf. also Supporting Information, Table SI-7). However, if only the CF energies of states arising from the ground multiplet $^3\text{H}_4$ are fitted, this fit converges too. The resulting CF parameters of all these converging fits are also given in Supporting Information, Table SI-8. Again, the quartic CF parameter is dominant.

Within the framework of the above-mentioned fitting procedures of the calculated CF splitting patterns of $\text{An}(\text{COT})_2$ ($\text{An} = \text{Pa}, \text{U}$) the spin-orbit coupling parameters ζ_{5f} of $\text{An}(\text{COT})_2$ and the Slater parameters F^2 , F^4 , and F^6 of $\text{U}(\text{COT})_2$ were fitted too. The ζ_{5f} parameters of $\text{Pa}(\text{COT})_2$ move between 887 and 1418 cm^{-1} , and those of $\text{U}(\text{COT})_2$ ^{137,143} have values of 1630 cm^{-1} and 2055 cm^{-1} (Supporting Information, Table SI-8). In the case of more salt-like An^{IV} compounds such as AnCl_4 , $\text{ThCl}_4:\text{An}^{4+}$, $\text{ThBr}_4:\text{An}^{4+}$, $[\text{NEt}_4]_2\text{AnX}_6$ ($\text{X} = \text{F}, \text{Cl}, \text{Br}, \text{I}$) ζ_{5f} moves between 1508 and 1533 cm^{-1} for $\text{An} = \text{Pa}$ ^{36,146–148} and between 1724 and 1970 cm^{-1} for $\text{An} = \text{U}$.^{36,149} Likewise, the Slater parameters fitted to the calculated CF splitting pattern of $\text{U}(\text{COT})_2$ as given in ref 143 ($F^2 = 86666 \text{ cm}^{-1}$, $F^4 = 43698 \text{ cm}^{-1}$, $F^6 = 81824 \text{ cm}^{-1}$) are far from those fitted to the experimental CF splitting patterns of molecular U^{IV} compounds such as $\text{Hf}(\text{BD}_4)_4:\text{U}^{4+}$,¹⁵⁰ Cp_3UCl ,¹⁰³ $[\text{Cp}_3\text{U}$

$(\text{NCS})_2]^-$,¹⁵¹ and $[\text{Cp}_3\text{U}(\text{NCBH}_3)_2]^{-151}$ ($41121 \text{ cm}^{-1} \leq F^2 \leq 45609 \text{ cm}^{-1}$, $37679 \text{ cm}^{-1} \leq F^4 \leq 46116 \text{ cm}^{-1}$, $19446 \text{ cm}^{-1} \leq F^6 \leq 28028 \text{ cm}^{-1}$).

The CF calculation for $[(\text{COT})\text{U}(\text{I})_2(\text{THF})_2]$ leads to the energetic sequence $E(|\pm 3\rangle) < E(|\pm 2\rangle) < E(|0\rangle) < E(|\pm 1\rangle) < E(|\pm 4\rangle)$ of the ground multiplet $^3\text{H}_4$, which corresponds to the calculated sequences for $\text{U}(\text{COT})_2$ given in refs 142, 143 but not for refs 69, 136–140. However, almost each of these calculations predicts that the lowest CF state is $|\pm 3\rangle$ followed by the first excited state $|\pm 2\rangle$. This result was also concluded from a comparison of calculated and experimental μ^2 , μ_{\parallel}^2 , μ_{\perp}^2 , and $\mu_{\parallel}^2 - \mu_{\perp}^2$ values, which were extracted from susceptibility and NMR data of $\text{U}(\text{C}_8\text{H}_7\text{SiMe}_3)_2$.^{152,153}

3. Conclusions

In contrast to quasi-centrosymmetric, from the f electrons perspective, full sandwich complexes of the stoichiometries $\text{KLn}(\text{COT})_2$ and $\text{An}(\text{COT})_2$, the half-sandwich complexes of the types $(\text{COT})\text{Ln}(\text{scorpionate})$, $(\text{COT})\text{Ln}(\text{I})(\text{THF})_3$, and $(\text{COT})\text{U}(\text{I})_2(\text{THF})_2$ exhibit f-f transitions of induced electric dipole character. For this reason, the CF splitting patterns of these compounds can be extracted from optical spectra. Accepting the argument that the observed optical spectra of $(\text{COT})\text{Ln}(\text{scorpionates})$ are mainly due to the $[\text{Ln}(\text{COT})]^+$ moiety, and that the additional scorpionate ligand causes only a weak distortion of the main field of $C_{\infty v}$ symmetry, truncated CF splitting patterns of the $[\text{Ln}(\text{COT})]^+$ ($\text{Ln} = \text{Pr}, \text{Nd}, \text{Sm}$) moiety could be derived and simulated by fitting the free parameters of a phenomenological Hamiltonian. The CF strength associated with one η^8 bonded COT ligand in $[\text{Ln}(\text{COT})]^+$ is somewhat weaker than that of three substituted η^5 bonded Cp' ligands in $\text{Ln}(\text{Cp}')_3$ ($\text{Cp}' = \text{C}_5\text{Me}_4\text{H}, \text{C}_5\text{H}_4\text{tBu}, \text{C}_5\text{H}_4\text{SiMe}_3$) but stronger than that of three $[\text{CH}(\text{SiMe}_3)_2]^-$ ligands in $\text{Ln}[\text{CH}(\text{SiMe}_3)_2]_3$. Likewise, the nephelauxetic effects associated with $(\text{COT})\text{Ln}(\text{scorpionates})$ are comparatively strong, indicating a non-negligible covalency of the bonds between f electrons and the COT ligand. The low energies of the pair of transitions between the lowest d level of Ce complex **5** and the multiplets $^2\text{F}_{5/2}$ and $^2\text{F}_{7/2}$, respectively, imply a strong interaction of 5d orbitals with the COT and scorpionate ligands. The even lower energies of the homoleptic full sandwich complex $\text{Li}(\text{THF})_4[\text{Ce}(\text{COT})_2]$ and the noticeably higher values of homoleptic $\text{Ce}(\text{Tp})_3$ demonstrate that the d orbitals are much more affected by the COT than the Tp ligand. This experimental finding does not agree with the results of model calculations on $\text{Pa}(\text{COT})_2$ and $\text{U}(\text{COT})_2$, where an essentially non-bonding $6d_{\sigma}$ orbital is predicted. Multiplying the CF parameters of $[\text{Pr}(\text{COT})]^+$ by a factor of 3 and using the free ion parameters of Cp_3UCl ,¹⁰³ a set of starting parameters was obtained which allowed, after some refinements, the simulation of the CF splitting pattern of $(\text{COT})\text{UI}_2(\text{THF})_2$ in a satisfactory manner. Although we have no experimental

(146) Amberger, H.-D.; Grape, W.; Stumpp, E. *Lawrence Berkeley Laboratory Report* **1981**, 12441, 89.

(147) Krupa, J. C.; Hussonnois, M.; Genet, M.; Guillaumont, R. *J. Chem. Phys.* **1982**, *77*, 154.

(148) Krupa, J. C.; Hubert, S.; Foyentin, M.; Edelstein, N. *J. Chem. Phys.* **1983**, *78*, 2175.

(149) Delamoye, P.; Rajnak, K.; Genet, M.; Edelstein, N. *Phys. Rev. B* **1983**, *28*, 4923.

(150) Rajnak, K.; Gamp, E.; Shinomoto, R.; Edelstein, N. *J. Chem. Phys.* **1984**, *80*, 5942; and references therein.

(151) Amberger, H.-D.; Reddmann, H.; Shalimoff, G. V.; Edelstein, N. M. *Inorg. Chim. Acta* **1987**, *139*, 335.

(152) Amberger, H.-D. *J. Less-Common Met.* **1983**, *93*, 235.

(153) Jahn, W.; Yünlü, K.; Oroschin, W.; Amberger, H.-D.; Fischer, R. D. *Inorg. Chim. Acta* **1984**, *95*, 85.

validation for the correctness of the assignments in the framework of the fitting procedure, the parameters used might be realistic as recent model calculations for $\text{Pa}(\text{COT})_2$ and $\text{U}(\text{COT})_2$ lead to CF parameters approximately twice as large as those for $(\text{COT})\text{UI}_2(\text{THF})_2$ (Supporting Information, Table SI-7).

Clearly, modern approximations describing the CF interaction of actinocenes are satisfactory; however, the values of the free ion parameters are significantly different from those of more ionic Pa^{IV} or U^{IV} compounds, or those of molecular complexes of U^{IV} .

It would be highly desirable that theorists calculate the electronic structures of half-sandwich complexes of the types $[\text{Ln}(\text{COT})]^+$ and $[\text{An}(\text{COT})]^{2+}$, where the predicted MO schemes can be checked by optical spectroscopy. To confirm the presented results, we plan to parametrize the CF splitting patterns of additional $(\text{COT})\text{LnX}$, $(\text{COT})\text{UX}_2$ and $(\text{COT})\text{UXY}$ complexes, where the ligands X, Y are associated with low CF strengths.

Acknowledgment. The authors thank Dr. N. M. Edelstein (Lawrence Berkeley National Laboratory) for running the presented susceptibility data, Dr. G. Kneer (Varian) for recording the excitation spectra, Prof. M. Dolg (Universität zu Köln) for a preliminary notification on the calculated CF splitting pattern (MRCISD) of $\text{U}(\text{COT})_2$, Dr. M. Ephritikhine (CNRS, Gif-sur-Yvette) for a donation of $(\text{COT})\text{UI}_2(\text{THF})_2$, and Prof. J. Takats (University of Alberta) for helpful discussions. Generous financial support by the Deutsche Forschungsgemeinschaft (SPP 1166 “Lanthanoid-spezifische Funktionalitäten in Molekül und Material”), the Fonds der Chemischen Industrie, and the Otto-von-Guericke-Universität Magdeburg is also gratefully acknowledged.

Supporting Information Available: Further details are given in Tables SI-1–SI-8 and Figures SI-1–SI-5, and crystallographic data in CIF format. This material is available free of charge via the Internet at <http://pubs.acs.org>.

IC801765N